

Supplemental Material

Supplemental Methods

Supplemental Figure 1. Histological analysis of the liver in WT mice pretreated with RIF followed by RTV.

Supplemental Figure 2. Effects of RIF on the expression of PXR target genes in the liver of hPXR/CYP3A4 mice.

Supplemental Figure 3. Histological analysis of the liver in hPXR/CYP3A4 mice pretreated with RIF followed by RTV.

Supplemental Figure 4. Effects of RIF on the expression of PXR target genes in the liver of hPXR/Cyp3a-null mice.

Supplemental Figure 5. Roles of human PXR and CYP3A4 in the hepatotoxicity associated with lead-in treatment with EFV followed by RTV.

Supplemental Figure 6. Effects of RTV on RIF metabolism and disposition in hPXR/CYP3A4 mice.

Supplemental Figure 7. RIF-mediated PXR activation and CYP3A4 induction increase RTV metabolism and bioactivation.

Supplemental Figure 8. Oxidative stress in the liver of hPXR/CYP3A4 and hPXR/Cyp3a-null mice pretreated with EFV followed by RTV.

Supplemental Figure 9. ER stress in the liver of hPXR/CYP3A4 and hPXR/Cyp3a-null mice pretreated with EFV followed by RTV.

Supplemental Table 1. Primers for qPCR analysis.

Supplemental Methods

Chemicals and reagents. Ritonavir (RTV) and rifampicin (RIF) were purchased from Sigma-Aldrich (St. Louis, MO). Efavirenz (EFV) was purchased from TCI Chemical (Portland, OR). The solvents for metabolite analysis were of the highest grade commercially available.

Animals and treatment. The *PXR*- and *CYP3A4*-humanized mouse models were developed based on previously generated hPXR, TgCYP3A4/hPXR, and *Cyp3a*-null mouse models (1-3). In brief, *CYP3A4* transgenic mice were generated by bacterial artificial chromosome (BAC) transgenesis, which contains the complete *CYP3A4* and *CYP3A7* genes including PXR response element (PXRE) (3). In *Cyp3a*-null mice, all eight *Cyp3a* genes were eliminated (1). TgCYP3A4/hPXR mice were crossed with *Cyp3a*-null mice to generate a mouse model expressing human *PXR* and *CYP3A4*, but deficient in the mouse *Pxr* and *Cyp3a* genes (hPXR/CYP3A4). In addition, *Cyp3a*-null mice were crossed with hPXR mice to generate a mouse model expressing human *PXR*, but deficient in the human *CYP3A4* gene and the mouse *Pxr* and *Cyp3a* genes (hPXR/*Cyp3a*-null). hPXR/CYP3A4 and hPXR/*Cyp3a*-null mice (3 weeks old) were verified by PCR genotyping of human *PXR* and *CYP3A4*, and mouse *Pxr* and *Cyp3a*. In addition, quantitative PCR (qPCR) and/or Western blotting were used to determine the expression of PXR target genes including CYP3A4. To determine the roles of PXR and CYP3A4 in RTV hepatotoxicity, WT, hPXR/CYP3A4, and hPXR/*Cyp3a*-null mice (male, 2-4 months old) were treated with RIF (50 mg in 1 kg diet) or EFV (500 mg in 1 kg diet) for seven days. On the eighth day, the mice were administered 50 mg/kg of RTV (two doses, ip) or corn oil (vehicle). All mice were killed on the ninth day and blood and liver samples collected for evaluation of liver injury.

Assessment of liver injury. Alanine transaminase (ALT) and aspartate transaminase (AST) levels in serum were analyzed by standard assays according to the kit procedures (Point Scientific Inc, Canton, MI). Sections of liver tissues were fixed in 4% formaldehyde phosphate solution overnight for histological analysis. Dehydration of fixed liver tissues was achieved by passing them through an increasing gradient of alcohol and then xylene solutions. Liver tissues were then embedded in paraffin and 4 μm sections were cut and stained with hematoxylin and eosin (H&E). For transmission electron microscopy (TEM), fresh liver samples ($\sim 1 \text{ mm}^3$) were placed into Karnovsky's fixative (2.5% glutaraldehyde and 2% paraformaldehyde). The liver samples were further processed using 1% osmium tetroxide, phosphate buffered saline and gradients of ethanol (30-100%) solution. Afterward, the liver tissues were kept overnight in Epon/propylene oxide solution (1:1), and then embedded and sectioned for TEM imaging.

Cell-based reporter assay of human PXR activation. The effects of RIF and EFV on human PXR activation were examined in the DPX2 cell line (Puracyp Inc., Carlsbad, CA), which was derived from HepG2 cells by stable transfection of human *PXR* cDNA and a luciferase reporter gene. Briefly, DPX2 cells were cultured in a 96-well plate with a density of 2×10^5 cells/ml. Ten μM RIF or EFV were incubated in DPX2 cells for 24 h followed by analysis of luciferase activity. The experiments were conducted in triplicate.

qPCR analysis. Total mRNA was extracted from 50 mg of liver tissues using TRIzol reagent (Invitrogen, Carlsbad, CA). Complementary DNA (cDNA) was made from 1 µg of total RNA with a SuperScript II Reverse Transcriptase kit and random oligonucleotides (Invitrogen, Carlsbad, CA). PCR primers (Table S1) were obtained from the Primer Bank (<http://pga.mgh.harvard.edu/primerbank/>) or designed by the Primer blast-NCBI-NIH (<https://www.ncbi.nlm.nih.gov/tools/primer-blast/>). qPCR was carried out using 25 ng cDNA, 150 nM of each primer, and 5 µL of SYBR Green PCR Master Mix (Applied Biosystems, Foster City, CA) in a total volume of 10 µL. The qPCR plate was analyzed on an ABI-Prism 7500 Sequence Detection System (Applied Biosystems, Foster City, CA). Cyclophilin was used as the housekeeping gene and the values were calculated using the comparative CT method.

Western blotting. Microsomal or total liver protein was used for blotting. Microsomal protein was prepared by homogenizing liver tissues in ice-cold buffer A (0.1 M phosphate buffer pH 7.5, sucrose 0.25 M, KCL 0.154 M). Liver homogenates were centrifuged at 12,100 g for 25 min at 4 °C and the resulting supernatant was spun at 38,100 g for 1 h. Microsomal pellets were re-suspended in buffer B (0.1 M phosphate buffer saline and 20% glycerol). For total protein, liver tissue was homogenized in ice-cold Ripa buffer (150 mM NaCl, 1.0% IGEPAL CA-630, 0.5% sodium deoxycholate, 0.1% SDS, 50 mM Tris, pH 8.0). The resulting homogenates were centrifuged at 10,000 g for 10 min and the supernatants were collected. Protein concentration was measured using the Bio-Rad protein assay (Hercules, CA). Twenty µg of protein from each sample was resolved on a 10% SDS-polyacrylamide gel electrophoresis. Proteins were electrophoretically transferred to PVDF membranes and probed using primary antibodies against Chop (Cell Signaling Technology, #2895S), Bip (Cell Signaling Technology, #3177S), CYP3A4 (Laboratory of Metabolism, NCI, #275-1-2), and Gapdh (EMD Millipore, #MAB374). Immunoreactive proteins were identified by a chemiluminescence detection method.

Effects of RTV on RIF metabolism. hPXR/CYP3A4 mice were treated with RIF (10 mg/kg, po) or RIF plus RTV (50 mg/kg, ip). Eighteen h after the treatment, the liver and feces were collected for analysis of RIF and its metabolite. In brief, liver and feces were weighed and homogenized in water (100 mg of liver in 400 µL of water and 100 mg of feces in 1000 µL of water). One hundred µL of the liver homogenate was mixed with 200 µL of acetonitrile to methanol (1:1 v/v) followed by vortexing. For feces, 100 µL of the homogenate was mixed with 200 µL of acetonitrile followed by vortexing. The samples were then centrifuged twice at 15,000 g for 10 min and the supernatants were transferred to the autosampler vials for metabolite analysis by ultra-performance liquid chromatography (UPLC) coupled with quadrupole time-of-flight mass spectrometry (QTOFMS) system (Waters Corporation, Milford, MA).

Effects of RIF on RTV metabolism. The effects of RIF on RTV metabolism were determined using mouse liver microsomes from hPXR/CYP3A4 and hPXR/Cyp3a-null mice pretreated with or without RIF for seven days. Incubations were conducted in 1 × phosphate buffered saline (PBS, pH 7.4) containing 10 µM RTV and 0.2 mg MLM in a final volume of 95 µL. After 5 min of pre-incubation at 37 °C, the reaction was initiated by the addition of 5 µL of 20 mM NADPH and continued for 40 min with gentle shaking. Incubations were terminated by adding 100 µL of

acetonitrile followed by vortexing for 30 s and centrifuging at 15,000 g for 10 min. Each supernatant was transferred to an autosampler vial for metabolite analysis by UPLC-QTOFMS.

UPLC-QTOFMS analysis. Metabolite separation was performed on an Acquity UPLC BEH C18 column (2.1 × 100 mm, 1.7 μm; Waters Corporation, Milford, MA). The flow rate of the mobile phase was 0.5 ml/min using a gradient ranging from 2% to 98% acetonitrile/water containing 0.1% formic acid. The column temperature was maintained at 50 °C. QTOFMS was operated in positive mode with electrospray ionization. MS data were acquired over a range of 50-1000 Da in centroid format. Tandem mass fragmentation with collision energy ramping from 15 to 45 eV was used for structural elucidations of metabolites.

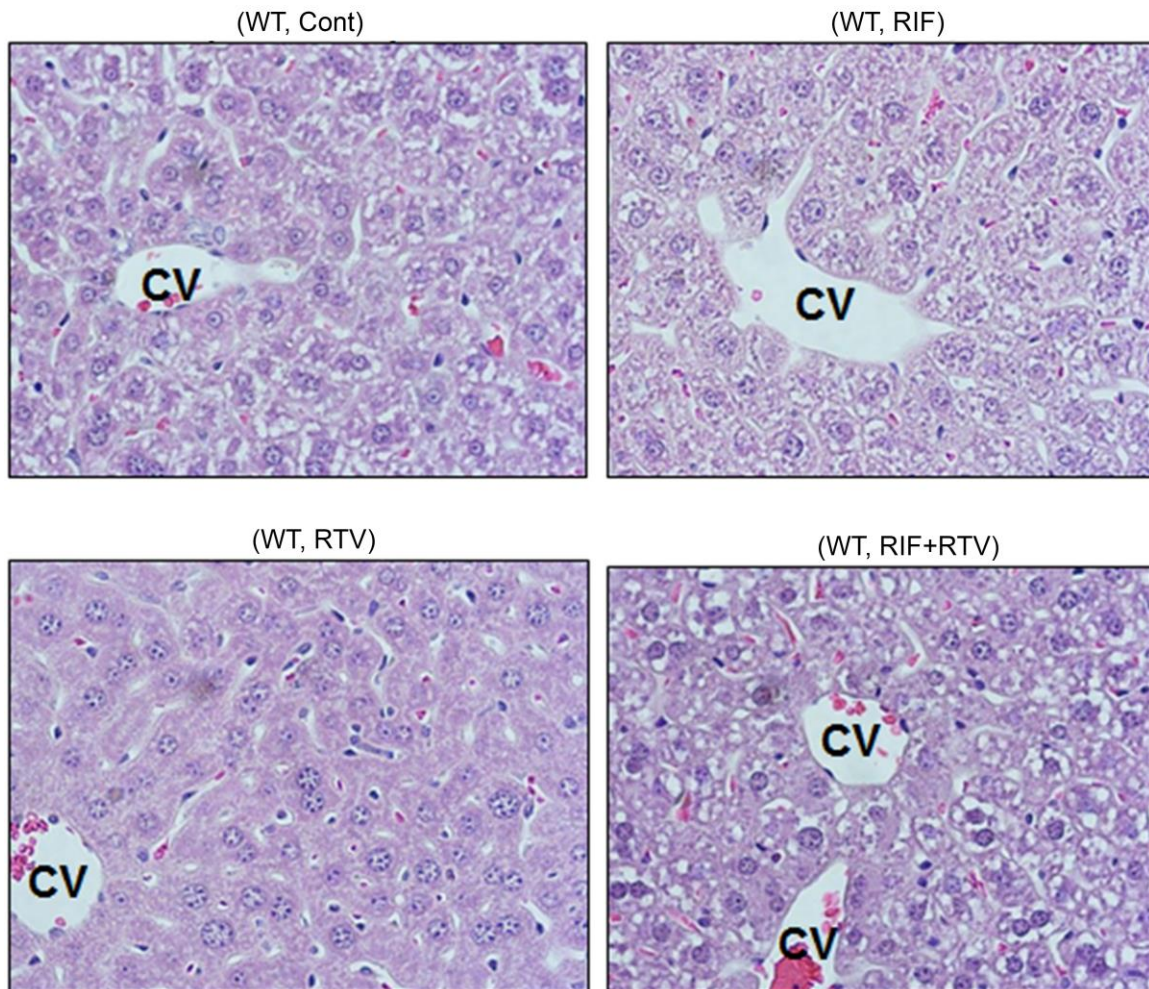
Liver metabolomics. Liver metabolome was analyzed in hPXR/CYP3A4 mice treated with vehicle, RIF, RTV, or RIF plus RTV. Briefly, liver samples were weighed and homogenized in water (100 mg of tissues in 500 μL of water). Two hundred μL of acetonitrile: methanol (1:1, v/v) was added to 100 μL of each homogenate, followed by vortexing and centrifugation at 15,000 g for 10 min. The supernatant was transferred to a new Eppendorf vial for a second centrifugation at 15,000 g for 10 min, and then transferred to an autosampler vial for metabolite analysis by UPLC-QTOFMS. A data matrix, including retention time and m/z, was generated through alignment of all the samples using MarkerLynx software (Waters, Milford, MA). The data matrix was further exported into SIMCA-P+ software (Version 13, Umetrics, Kinnelon, NJ). Principal component analysis (PCA) and orthogonal partial least-squares discriminant analysis (OPLS-DA) were conducted to maximize the class discrimination. The metabolites that significantly contributed to the discrimination between groups were subjected to structure identification.

References

1. van Herwaarden AE, Wagenaar E, van der Kruijssen CM, van Waterschoot RA, Smit JW, Song JY, et al. Knockout of cytochrome P450 3A yields new mouse models for understanding xenobiotic metabolism. *J Clin Invest.* 2007;117(11):3583-92.
2. Ma X, Shah Y, Cheung C, Guo GL, Feigenbaum L, Krausz KW, et al. The pregnane X receptor gene-humanized mouse: a model for investigating drug-drug interactions mediated by cytochromes P450 3A. *Drug Metab Dispos.* 2007;35(2):194-200.
3. Ma X, Cheung C, Krausz KW, Shah YM, Wang T, Idle JR, et al. A double transgenic mouse model expressing human pregnane X receptor and cytochrome P450 3A4. *Drug Metab Dispos.* 2008;36(12):2506-12.

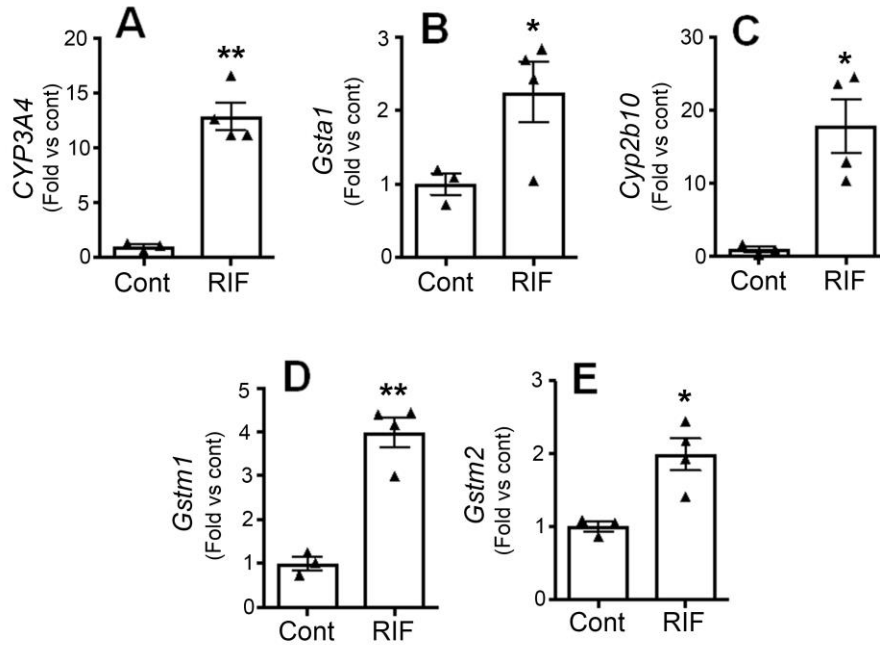
Figure legends

Supplemental Figure 1



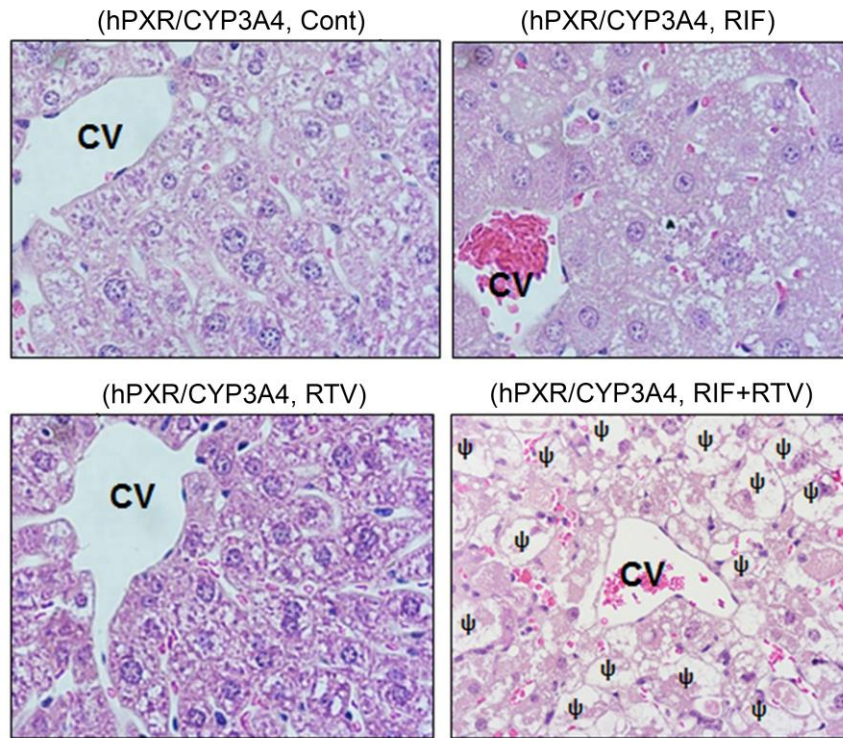
Supplemental Figure 1. Histological analysis of the liver in WT mice pretreated with RIF for seven days followed by RTV. H&E staining; CV, central vein; original magnification 400X.

Supplemental Figure 2



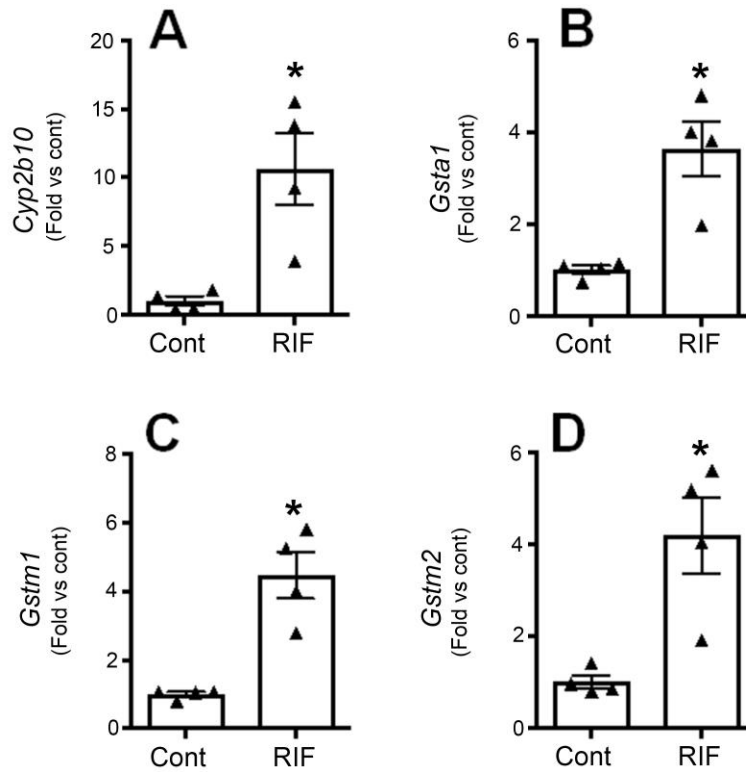
Supplemental Figure 2. Effects of RIF on the expression of PXR target genes in the liver of hPXR/CYP3A4 mice. Mice were treated with RIF for seven days. *CYP3A4* (A), *Cyp2b10* (B), *Gsta1* (C), *Gstm1* (D), and *Gstm2* (E) mRNAs were analyzed by qPCR. All data are expressed as means \pm S.E.M. ($n = 3-4$). The data in control groups were set as 1. Statistical significance was determined by two tailed unpaired t-test. * $P < 0.05$, ** $P < 0.01$ vs control.

Supplemental Figure 3



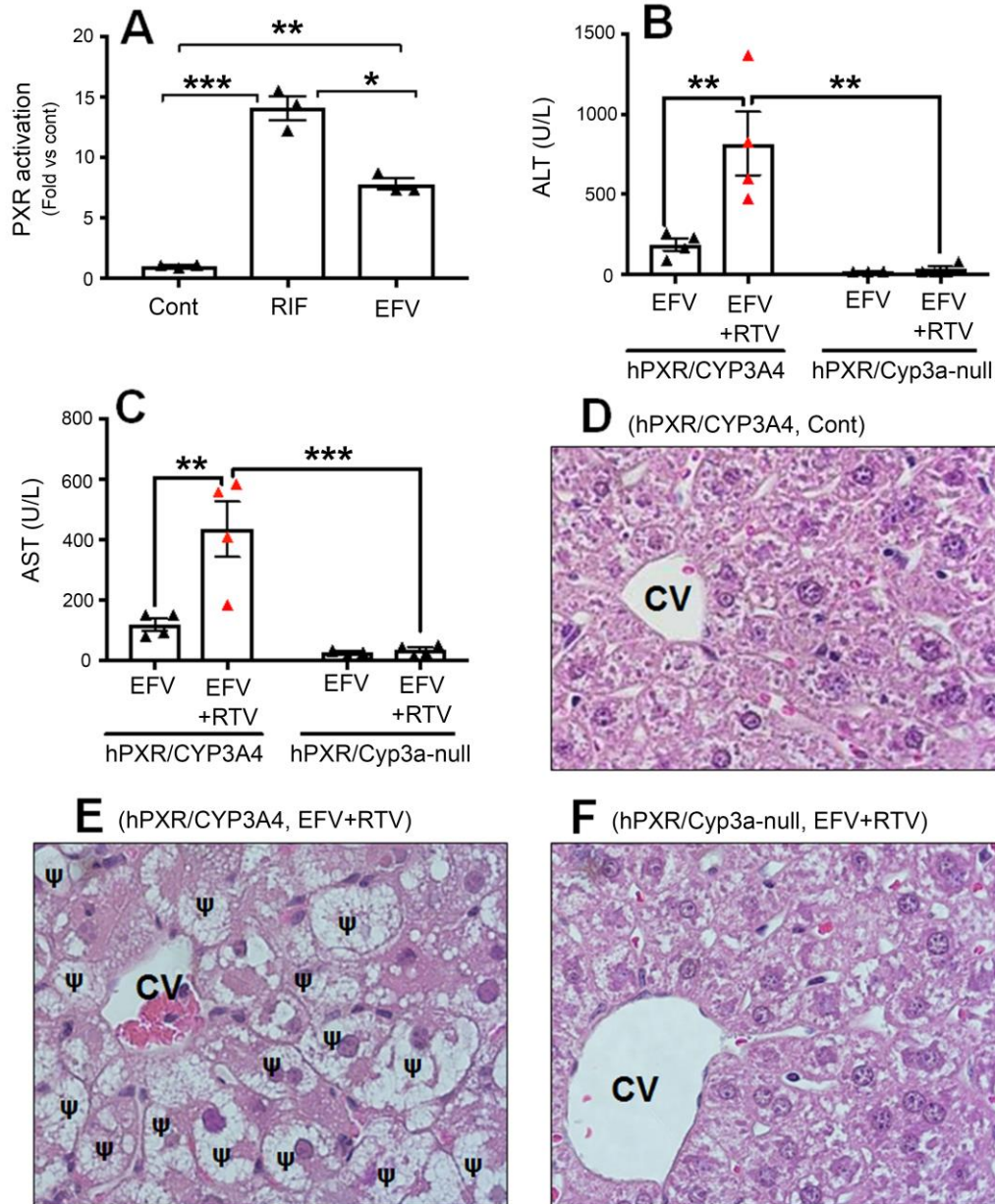
Supplemental Figure 3. Histological analysis of the liver in hPXR/CYP3A4 mice pretreated with RIF for seven days followed by RTV. H&E staining; CV, central vein; ψ indicates hepatocyte degeneration; original magnification 400X.

Supplemental Figure 4



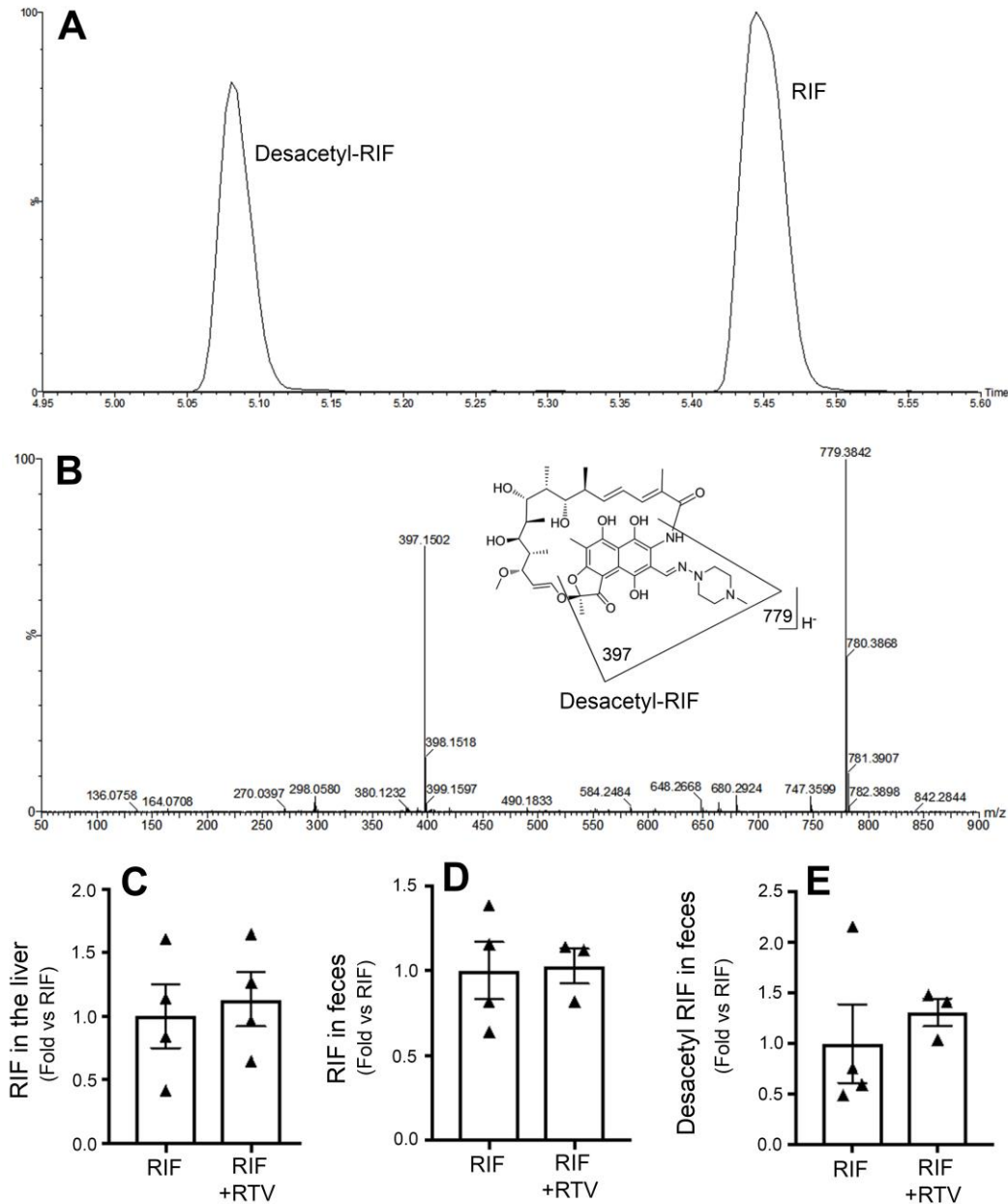
Supplemental Figure 4. Effects of RIF on the expression of PXR target genes in the liver of hPXR/Cyp3a-null mice. Mice were treated with RIF for seven days. *Cyp2b10* (A), *Gsta1* (B), *Gstm1* (C), and *Gstm2* (D) mRNAs were analyzed by qPCR. All data are expressed as means \pm S.E.M. ($n = 4$). The data in control groups were set as 1. Statistical significance was determined by two tailed unpaired t-test. * $P < 0.05$ vs control.

Supplemental Figure 5



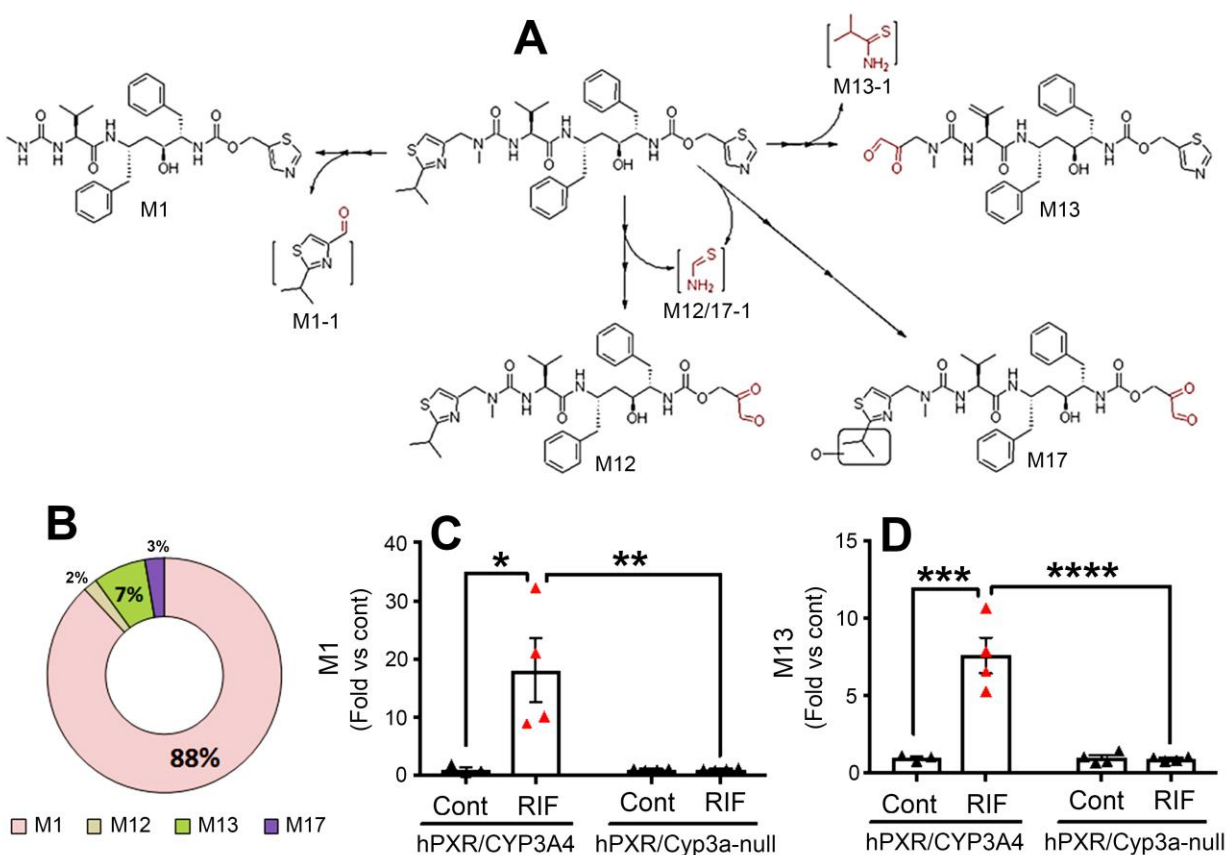
Supplemental Figure 5. Roles of human PXR and CYP3A4 in the hepatotoxicity associated with lead-in treatment with EFV followed by RTV. (A) Effect of EFV (10 μ M) on PXR activation in a cell-based reporter assay ($n = 3$). The data in control group were set as 1. RIF (10 μ M) was used as a positive control. (B-F) Evaluation of liver damage in hPXR/CYP3A4 and hPXR/Cyp3a-null mice pretreated with EFV for seven days followed by RTV. (B, C) Activities of ALT and AST in the serum. All data are expressed as means \pm S.E.M. ($n = 4$). Statistical significance was determined by One or two-way ANOVA with Tukey's post hoc test. * $P < 0.05$, ** $P < 0.01$, *** $P < 0.001$. (D-F) Histological analysis of liver. H&E staining; CV, central vein; ψ indicates hepatocyte degeneration; original magnification 400X.

Supplemental Figure 6



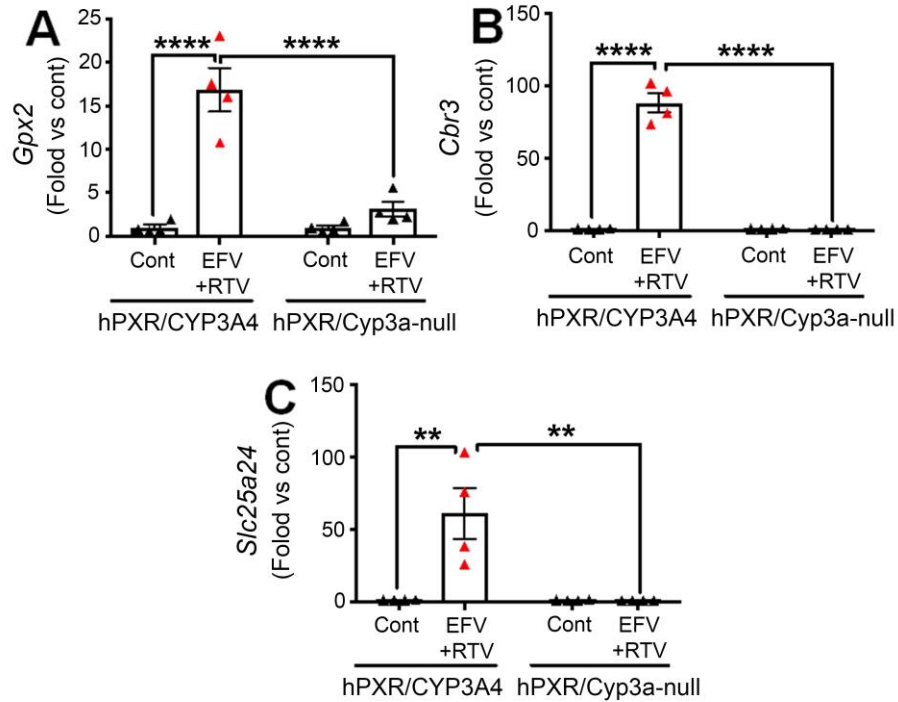
Supplemental Figure 6. Effects of RTV on RIF metabolism and disposition in hPXR/CYP3A4 mice. Feces and liver samples were collected overnight after treatment with RIF or RIF plus RTV. RIF and its metabolite desacetyl-RIF were analyzed by UPLC-QTOFMS. (A) Extracted chromatograms of RIF and desacetyl-RIF from feces. (B) MS/MS spectrum of desacetyl-RIF. The structure of desacetyl-RIF with fragmental patterns is inlaid in the spectra. (C) The relative abundance of RIF in the liver. (D) The relative abundance of RIF in feces. (E) The relative abundance of desacetyl-RIF in feces. All data are expressed as means \pm S.E.M. ($n = 3-4$). The data in RIF group were set as 1. Statistical significance was determined by two tailed unpaired t-test.

Supplemental Figure 7



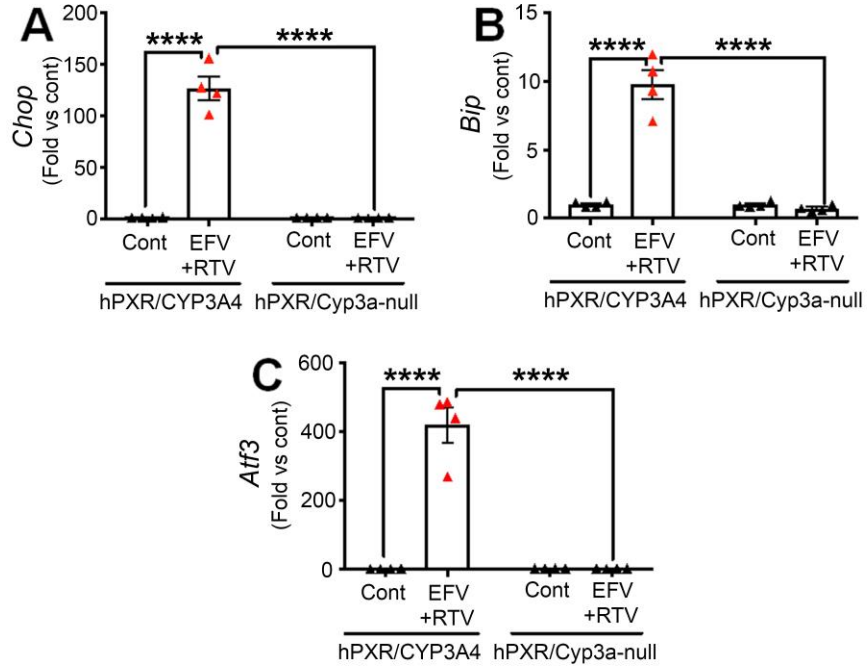
Supplemental Figure 7. RIF-mediated PXR activation and CYP3A4 induction increase RTV metabolism and bioactivation. (A) A scheme showing the bioactivation pathways of RTV. (B) Relative abundances of M1, M12, M13, and M17 produced in the liver microsomes of hPXR/CYP3A4 mice pretreated with RIF for seven days. These metabolites were analyzed by UPLC-QTOFMS and the total peak areas of these 4 metabolites were set as 100%. M1 was identified as the most abundant metabolite followed by M13. (C, D) Production of M1 and M13 in the liver microsomes of hPXR/CYP3A4 and hPXR/Cyp3a-null mice pretreated with or without RIF for seven days. The data are expressed as means \pm S.E.M. ($n = 3-4$). The data in control groups of hPXR/CYP3A4 mice were set as 1. Statistical significance was determined by two-way ANOVA with Tukey's post hoc test. * $P < 0.05$, ** $P < 0.01$, *** $P < 0.001$, **** $P < 0.0001$.

Supplemental Figure 8



Supplemental Figure 8. Oxidative stress in the liver of hPXR/CYP3A4 and hPXR/Cyp3a-null mice pretreated with EFV for seven days followed by RTV. *Gpx2* (A), *Cbr3* (B), and *Slc25a24* (C) mRNAs were analyzed by qPCR. All data are expressed as means \pm S.E.M. ($n = 4$). The data in the control group of hPXR/CYP3A4 mice were set as 1. Statistical significance was determined by two-way ANOVA with Tukey's post hoc test. ** $P < 0.01$, **** $P < 0.0001$.

Supplemental Figure 9



Supplemental Figure 9. ER stress in the liver of hPXR/CYP3A4 and hPXR/Cyp3a-null mice pretreated with EFV for seven days followed by RTV. *Chop* (A), *Bip* (B), and *Atf3* (C) mRNAs were analyzed by qPCR. All data are expressed as means \pm S.E.M. ($n = 4$). The data in the control group of hPXR/CYP3A4 mice were set as 1. Statistical significance was determined by two-way ANOVA with Tukey's post hoc test. **** $P < 0.0001$.

Supplemental Table 1. Primers for qPCR analysis.

Gene	Forward 5' -3'	Reverse 3'-5'
Atf3	GAGGATTTTGCTAACCTGACACC	TTGACGGTAACTGACTCCAGC
Bax	TCCCCCGAGAGGTCTTTT	CGGCCCCAGTTGAAGTTG
Bip	AGTGGTGGCCACTAATGGAG	CAATCCTTGCTTGATGCTGA
Cbr3	GGCACTCCGGTTAAGTAACTC	TGTCACTTGGTCGAATTTGTTCA
Chop	CTGCCTTTCACCTTGGGAC	CGTTTCCTGGGGATGAGATA
Cyp2b10	GGGAAAGCGCATTGTCTTG	GATGGACGTGAAGAAAAGGAACA
Dr5	ATAAAAAGAGGGCTGTGAACGGG	GGTCCAAGAGAGACGA
Gpx2	GCCTCAAGTATGTCCGACCTG	GGAGAACGGGTCATCATAAGGG
Gsta1	GCAGGGGTGGAGTTTGAAGA	CAGGGCTCTCTCCTTCATGTC
Gstm1	GAGGATCCGTGCAGACATT	ACTCTGGCTTCTGCTTCTCA
Gstm2	TGACTACATGAAGAGCAGCCG	CTTTGGGTTCAAAAGGCCA
Mcp1	CAACTCTCACTGAAGCCAGCTCT	CAGGCCCAGAAGCATGACA
Slc25a24	AGGCTTTCGGCAGATGGTAAA	CCTTCCTCGGTAAGCAACTTCT